Indian Journal of Engineering & Materials Sciences
Vol. 15, February 2008, pp. 55-60

Synthesis and characterization of $Mn_{0.4}Zn_{0.6}Al_{0.1}Fe_{1.9}O_4$ nano-ferrite for high frequency applications

Preeti Mathur, Atul Thakur* & M Singh

Material Science Laboratory, Department of Physics, Himachal Pradesh University, Shimla 171 005, India

Received 20 June 2007; accepted 30 January 2008

Nano-ferrite of composition $Mn_{0.4}Zn_{0.6}Al_{0.1}Fe_{1.9}O_4$ synthesized by co-precipitation method has been reported. The structural studies have been made by using X-ray diffraction (XRD) technique and scanning electron microscopy (SEM), which confirms the formation of single spinel phase and nanostructure. The dc resistivity is studied as a function of temperature and values are found about two times more than those for the samples prepared by the other chemical methods due to stoichiometric composition and better crystal structure of the ferrite. Even at nanolevel, the value of initial permeability is found to be 495 and low magnetic losses make these ferrites especially suitable for high frequency applications. The particle size is calculated using Scherrer's equation for Lorentzian peak, which comes out between 32-43 nm. Possible mechanisms contributing to these processes have been discussed.

Mn-Al-Zn ferrites are well known technological magnetic materials finding applications in various electrical and magnetic devices because of their high magnetic permeability and low core losses[1]. These ferrites have been widely used in electronic applications such as transformers, choke coils, noise filters and recording heads. Properties of ferrites are known to be sensitive to the processing technique[2], which are mainly solution techniques. In solution techniques, the chances of getting contamination from outside are negligible. Therefore, in the present work, non-conventional preparation technique, known as co-precipitation method, is used for the preparation of $Mn_{0.4}Zn_{0.6}Al_{0.1}Fe_{1.9}O_4$ ferrite. The main advantages of this method are that it is inexpensive, time saving and results in superior properties of ferrites processed at a much lower temperature. In our previous studies[3], we have optimized $Mn_{0.4}Zn_{0.6}Al_{0.1}Fe_{1.9}O_4$ ferrite from the long series of $Mn_{0.4}Zn_{0.6}Al_xFe_{2-x}O_4$ ferrite system for its better magnetic properties. Therefore, in the present work, a detailed study on $Mn_{0.4}Zn_{0.6}Al_{0.1}Fe_{1.9}O_4$ ferrite has been made.

Experimental Procedure

Mn-Al-Zn ferrite of composition $Mn_{0.4}Zn_{0.6}Al_{0.1}Fe_{1.9}O_4$ was prepared by the co-precipitation method. The materials used were manganese chloride (98% Merck, India), zinc chloride (96% Merck, India), aluminium chloride (99% Merck, India), iron (III) chloride (98% Merck, India) and sodium hydroxide (96% Merck, India). The experimental details are discussed elsewhere[4]. The residue obtained in this method is dried at 40°C and then, calcinated in a box type furnace at 200°C for 15 h at the rate of 200°C/h to obtain a ferrite powder. This powder was mixed with 2% PVA binder and pressed into pellets of 1.50 cm diameter and 0.20 cm thickness under a pressure of 10 tons (1 ton = 1.016×10^3 kg) and rings of 1.5 cm outer diameter, 1.0 cm inner diameter and 0.20 cm thickness under a pressure of 5 tons. These samples were sintered in air at 500°C at a heating rate of 100°C/h and were subsequently cooled. The pellets were coated with silver paste to provide electrical contacts and the rings were wound with about 50 turns of 32 SWG enameled copper wire to form torroids. The microstructure of the ferrite was studied by using scanning electron microscope (SEM) of JEOL-7400 FEGSEM & EDS (capable of 1 nm resolution). X-ray diffraction measurements were taken on a Rigaku Geiger Flex 3 kW diffractometer using CuK_α source. The initial permeability and loss factor were measured up to 30 MHz by using Agilent Technologies 4285A Precision LCR Meter. Resistivity as a function of temperature was measured by using Two-Probe method. The Curie temperature was measured by using gravity method.

Results and Discussion

X-ray diffraction pattern of the $Mn_{0.4}Zn_{0.6}Al_{0.1}Fe_{1.9}O_4$ ferrite sample pre-sintered at 200°C and sintered at 500°C are shown in Figs 1 and 2 respectively. The observed diffraction lines were

*For correspondence (E-mail: atulthakur@zapak.com)

found to correspond to those of standard pattern of manganese ferrite with no extra lines, indicating thereby that the samples have a single phase cubic spinel structure and no unreacted constituents were present in these samples. Lattice constant '*a*' for the samples sintered at 200°C and 500°C were calculated from the observed '*d*' values and found to be 8.412Å and 8.419Å respectively. These observations are in accordance with those reported in literature[5]. The peak becomes sharper with an increase in the sintering temperature.

Properties of ferrites are influenced by various factors such as compositional stoichiometry and microstructure, which in turn are strongly affected by the processing parameters[6]. In an ideal, stoichiometric, cubic spinel ferrite, the iron ions are required to be present primarily in the +3 oxidation state. However, during processing, there is a possibility of conversion of some Fe^{3+} ions to the +2 state. This conversion is mainly caused by the volatilization of zinc ions from the sample at high sintering temperatures[7]. Loss of zinc results in unsaturated oxygen ions. In order to restore charge neutrality in the ferrite, electron from oxygen are transferred to Fe^{3+}, thereby reducing them to Fe^{2+} and oxygen may be lost from the sample. These changes in the ferrite lead to deviations from lattice homogeneity and stoichiometry, which may affect the ferrite properties.

The particle size of the samples has been estimated from the broadening of the X-ray diffraction peaks using the Scherrer's equation[8] for Lorentzian peak:

$$d = \frac{0.9\lambda}{(w - w_1)\cos\theta} \quad \ldots (1)$$

where d is the grain diameter, w and w_1 are the half intensity width of the relevant diffraction peak and the instrumental broadening respectively, λ is the X-ray wavelength and θ is the angle of diffraction. The average particle size was found to be 32 nm at 200°C and 43 nm at 500°C, which is due to lack of domain magnetic structure in the samples[9]. Figures 3 and 4 show scanning electron micrograph of the sample sintered at 200°C and 500°C respectively, which are in good agreement with the theoretical XRD results. In small sized grains, there is a possibility of re-oxidation of Fe^{2+} to Fe^{3+} during cooling after the sintering process, as diffusion of oxygen advances

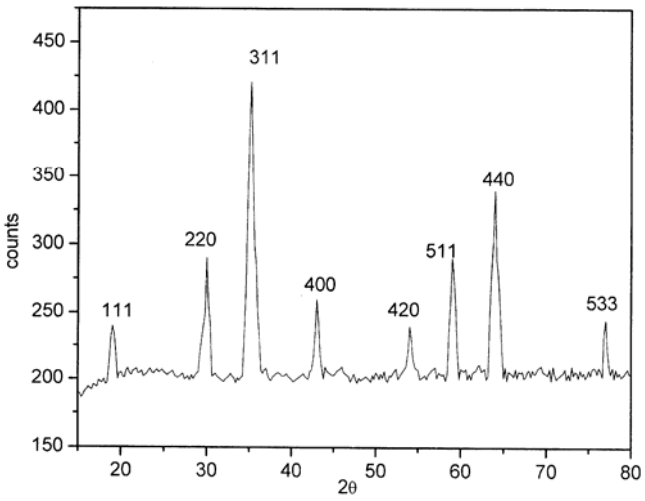

Fig. 1 — X-ray diffraction pattern of $Mn_{0.4}Zn_{0.6}Al_{0.1}Fe_{1.9}O_4$ sintered at 200°C for 15 h

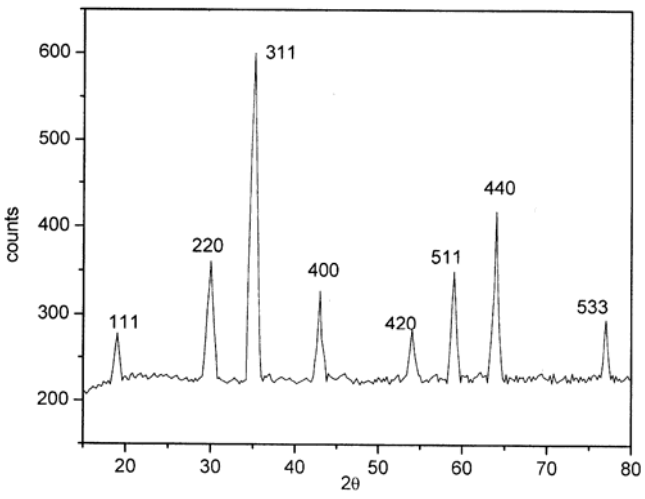

Fig. 2 — X-ray diffraction pattern of $Mn_{0.4}Zn_{0.6}Al_{0.1}Fe_{1.9}O_4$ sintered at 500°C for 15 h

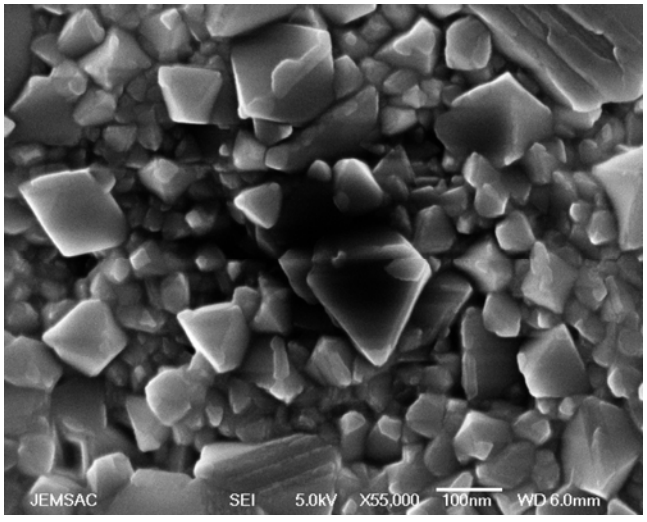

Fig. 3 — SEM of the fractured surface of $Mn_{0.4}Zn_{0.6}Al_{0.1}Fe_{1.9}O_4$ sintered at 200°C for 15 h

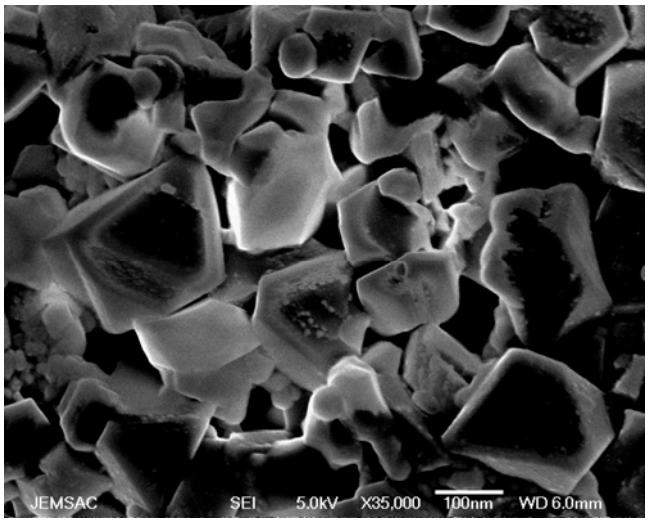

Fig. 4 — SEM of the fractured surface of $Mn_{0.4}Zn_{0.6}Al_{0.1}Fe_{1.9}O_4$ sintered at 500°C for 15 h

more rapidly in smaller grains than in larger ones. Re-conversion of Fe^{2+} to Fe^{3+} improves the ferrite stoichiometry[10].

The trends in the value of initial permeability, μ_i, with frequency were same at different temperatures as shown in Fig. 5. There is a decrease in the value of μ_i with an increasing frequency up to 10 MHz and a significant rise is observed at high frequencies. Initial permeability, μ_i , is found to be high as the sample is formed at a low temperature and the grain size is found to be small and uniform, which results in a single domain structure with uniform magnetization[9]. The resonance peak, which occurs when the frequency of applied field equals the Larmor precession of electron spins, could not be observed in the present technique. The main reason is that, as the grain size becomes smaller and uniform, the resonance character vanish[11]. Similar trend of results was found by Rado *et al.*[12] and Snoek[13]. The other reason for the absence of resonance peak may be as they probably lie beyond the measurable frequency range. The variation of initial permeability with frequency can be understood on the basis of Globus model[14]. According to this model, relaxation character,

$$(\mu_i - 1)^2 f_r = \text{constant} \quad \ldots (2)$$

where μ_i is the static initial permeability and f_r is the relaxation frequency. These researchers also showed that the transformation of magnetic spectra from the relaxation character to the resonance character changes Eq. (2) to

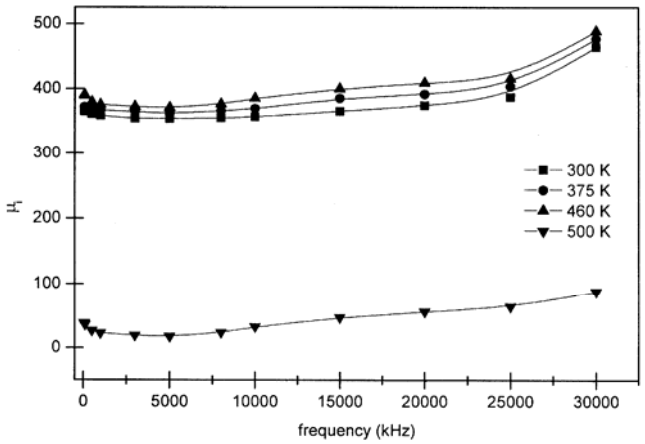

Fig. 5 — Variation of initial permeability, μ_i, with frequency at different temperatures

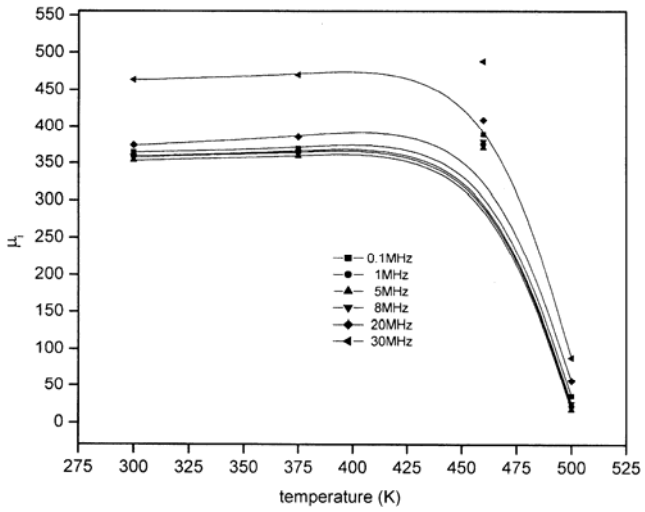

Fig. 6 — Variation of initial permeability, μ_i, with temperature at different frequencies

$$(\mu_i - 1)^{1/2} f_r = \text{constant} \quad \ldots (3)$$

It follows from this equation that the dispersion frequency is expected to be lower for specimen of higher permeability. At nanolevel, initial permeability of 495 is a good value. The initial permeability, μ_i , is found to be high as compared to that observed in the ferrite prepared by the soft chemical route[4].

The variation of initial permeability, μ_i, with temperature at different frequencies is shown in Fig. 6. The initial permeability, μ_i, is found to increase with an increase in temperature at all the frequencies, as is expected. At a temperature of 460 K, called the transition temperature, T_d, it attains a maximum value, after which there is a decrease in the initial permeability. This temperature was found in accordance with the Curie temperature, T_c (458 K),

obtained from the gravity method. The Curie temperature is the temperature above which the thermal agitation overcomes the alignment of magnetic moments and causes the material to become paramagnetic. It is typical of most magnetic materials that initial permeability, μ_i, increases with the rising temperature to a peak value just below the Curie temperature, T_c and decreases to μ_o above Curie temperature[15]. The sharp drop in the initial permeability at the Curie point indicates a good homogeneity in composition for the co-precipitation method.

The variation of permeability loss factor, $\tan\delta_\mu$, with frequency at different temperatures is given in Fig. 7. As can be seen, the values are of the order 10^{-2}-10^{-3} for different frequencies. These values are about the same and in some cases are of an order of magnitude lower than those for the specimens prepared by the soft chemical route[13]. The variation of $\tan\delta_\mu$ with frequency showed identical behaviour for all the specimens.

Figure 8 shows the variation of log ρ with 1/*T*. The resistivity of the sample decreases with the increasing temperature according to the relation $\rho = \rho_o e^{E\rho/kT}$, where E_ρ represents an activation energy[16] which is the energy needed to release an electron from the ion for a jump to the neighbouring ion, so giving rise to electrical conductivity. Upon an electron jump, a displacement occurs of the ions in the neighbourhood of the electron in question. Activation energy, E_ρ, was calculated from the slope of the graph given in Fig. 7 according to the relation:

$$E_\rho = 0.198 \times 10^{-3} \times d(\log \rho)/d(1/T) \quad \ldots(4)$$

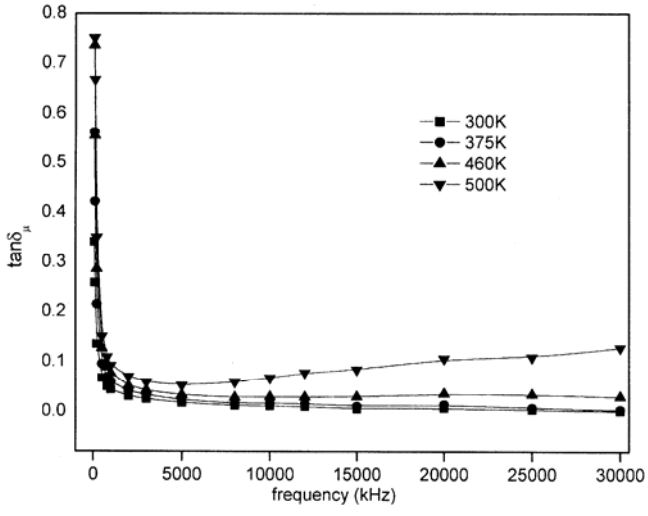

Fig. 7 — Variation of permeability loss factor, $\tan\delta_\mu$, with frequency at different temperatures

It is found that the value of activation energy in ferromagnetic region is lower than that of the paramagnetic region. The lower activation energy in the ferromagnetic region is attributed to the magnetic disordering[17]due to the decrease in concentration of current carriers[18], while the change in activation energy is attributed to the change in conduction mechanism[19]. Activation energy for the sample is found to be 0.3718 eV, which indicates that the ferrite formed is *p*-type semiconductor and the majority charge carrier are holes. The increase in resistivity is also attributed to the *p*-type conductivity, which increases the activation energy on the basis of Verwey conduction mechanism[16].

With the increase in temperature from 300 K to 500 K, dc resistivity is found to decrease from 78.2 × 10^6 Ωcm to 22.6 × 10^6 Ωcm as shown in Fig. 9. This value is about two times more than that of the ceramic ferrite[5]. This anomalous increase in resistivity is attributed to nano-structure of ferrite. This property makes these ferrites suitable for high frequency applications where eddy current losses become

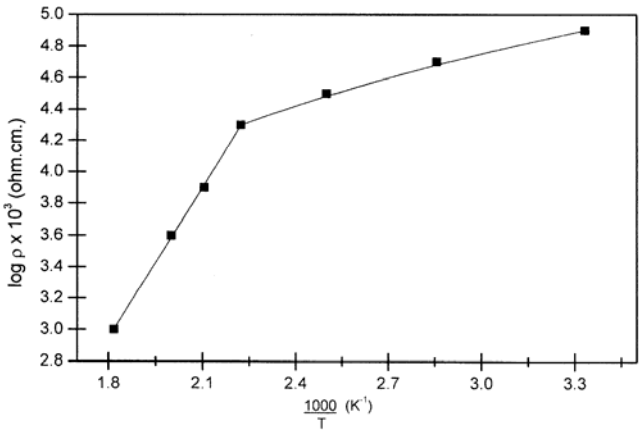

Fig. 8 — Plot of log ρ ×10^3 (ohm.cm) with 1000/*T* (K^{-1})

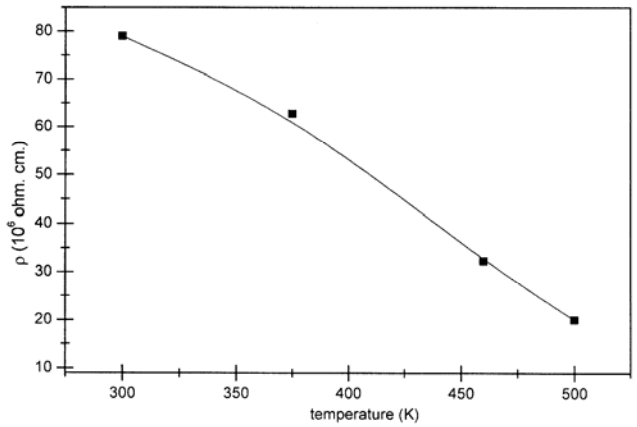

Fig. 9 — Variation of dc resistivity with temperature

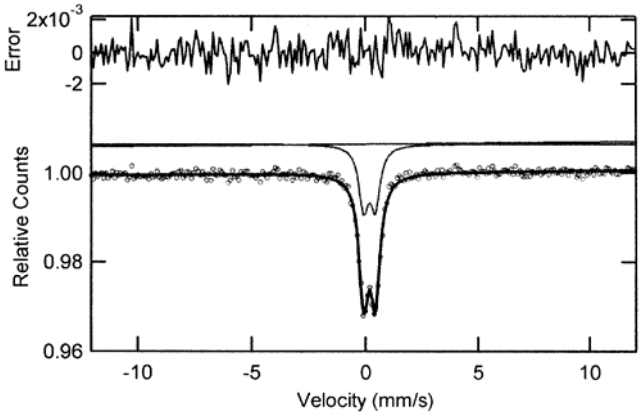

Fig. 10 — Room temperature Mössbauer spectrum for $Mn_{0.4}Zn_{0.6}Al_{0.1}Fe_{1.9}O_4$ ferrite sample sintered at 500°C

appreciable. The higher values of dc resistivity are because of stoichiometric compositions, uniform crystal structures and the improved nano-structures obtained by the co-precipitation method. Samples sintered at low temperature possess small grain size[4] because at high sintering temperature the grain growth takes place from nano to micro and nano-structure is lost. Sample with small grain consists of more number of grain boundaries. The grain boundaries are the region of mismatch between the energy states of adjacent grains and hence acts barrier to the flow of electrons. Another advantage of small grain size is that it helps in reducing Fe^{2+} ions as oxygen moves faster in small grains, thus keeping iron in Fe^{3+} state. Therefore, sample sintered at low temperature is found to exhibit high resistivity as compared to ceramic ferrite.

Figure 10 shows the room temperature Mössbauer spectrum for $Mn_{0.4}Zn_{0.6}Al_{0.1}Fe_{1.9}O_4$ ferrite sample sintered at 500°C. It can be seen from the figure that the sample shows a doublet type of Mössbauer spectra and no ferromagnetic nature, i.e., six line pattern of Mössbauer spectra, has been observed. Some spectral broadening is also observed. This spectral broadening is due to the changes in the tetrahedral bond length and due to the change in the Zn^{2+}, Mn^{2+}, Al^{3+} and Fe^{3+} ionic distributions in the tetrahedral and octahedral sites of this cubic spinel ferrite system[20]. From the experimental Mössbauer spectra, isomer shift (I.S.), quadrupole splitting (Q.S.) and FWHM has been calculated by a standard least square fitting program, NORMOSFIT. The values of I.S., Q.S and FWHM are 0.31 mm/s, 0.29mm/s and 0.51mm/s, respectively. The appearance of single quadrupole doublet in the Mössbauer spectra justifies the superparamagnetic behaviour of the nanoferrite. The superparamagnetic materials contain very small particles. The average particle size of these materials lies in nanometric range with single domain particle[21,22]. Therefore, the nanoferrites in the present study are single domain particles

Conclusions

Nano-structured $Mn_{0.4}Zn_{0.6}Al_{0.1}Fe_{1.9}O_4$ ferrite is successfully synthesized by using co-precipitation method. Hence, it is concluded that the initial permeability, μ_i, is a sensitive function of ambient temperature. It attains a maximum value at Curie temperature, T_c. In this method, we were successful in achieving high resistivity, which was about two times more as compared to the conventional method. Appreciable value of initial permeability was obtained at a low temperature and permeability loss factors were also found remarkably low. Co-precipitation technique is an effective and convenient route to synthesize nanocrystalline $Mn_{0.4}Zn_{0.6}Al_{0.1}Fe_{1.9}O_4$ ferrite particles because there is no requirement for a calcination process at high temperature. The synthesized powder has high activity due to its nanosized particle size. Ferrite sample can be sintered at 500°C and possesses a fine grained microstructure. The low temperature sintered $Mn_{0.4}Zn_{0.6}Al_{0.1}Fe_{1.9}O_4$ ferrite has good electromagnetic properties which makes this material suitable for high frequency applications.

Acknowledgement

The authors thank Dr Gari Harris, JEOL Analytical Electron Microscopy and Surface Analysis Centre, Department of Electronic Engineering and Physics, University of Dundee, for providing SEM facility and fruitful discussion during the study.

References

1 Rosales M I, Amano E, Cuautle M P & Valenzuela R, *Mater Sci Eng* B, 49 (1997) 221.
2 Thakur A & Singh M, *Ceram Int*, 29 (2003) 505-511.
3 Thakur A, Mathur P & Singh M, *Z Phys Chem*, 221 (2007) 837-845.
4 Thakur A, Mathur P & Singh M, *J Phys Chem Solids*, 68 (2007) 378-381.
5 Smit J & Wijn H P J, *Ferrites*, (Philips Technical Library, Eindhoven, Netherlands), 1959, 145.
6 Verma A, Goel T C, Mendiratta R G & Alam M I, *Mater Sci Eng* B, 60 (1999) 156.
7 Verma A, Goel T C & Mendiratta R G, *Mater Sci Technol*, 16 (2000) 712-715.
8 Cullity B D, *Elements of X-ray Diffraction* (Addison Wesley Reading, MA), 1978.
9 Caizer C & Stefanescu M, *Physica* B, 327 (2003) 129-134.

10 Smit J & Wijn H P J, *Ferrites* (Philips Technical Library, Eindhoven, Netherlands), 1959, 230.

11 Singh M, Ph D Thesis, Himachal Pradesh University, Shimla, India, 1996.

12 Rado G T, Wright R W & Emerson W H, *Phys Rev*, 80 (1960) 273.

13 Snoek J L, *New Developments in Ferromagnetic Materials* (Elsevier Publishing, New York) 1947.

14 Gieraltowski J & Globus A, *IEEE Trans Magn*, 13 (1977) 1359.

15 Soohoo R F, *Theory and Application of Ferrites* (Prentice-Hall, USA), 1960.

16 Verwey E J W, Haaijman P W, Romeyn F C & van Oosterhout G W, *Philips Res Rep*, 5173-187 (1950).

17 Barerner K, Mandal P & Helmolt R V, *Phys Status Solidi (B)*, 223 (2001) 811-820.

18 Baszsynski J, *Acta Phys Polym*, 35 (1969) 631.

19 Murthy V R K & Sobhandri J, *Phys Status Solidi (A)*, 38 (1977) 647.

20 Chakravarti M, Sanyal D & Chakravarti A, *J Phys Condens Mater,* 19 (2007) 236210.

21 Roy M K & Verma H C, *J Magn Magn Mater*, 306 (2006) 98-102.

22 Thakur A, Ph D Thesis, Himachal Pradesh University, Shimla, 2007.